Available online at www.sciencedirect.com
SCIENCE DIRECT
Thin Solid Films 506–507 (2006) 597 – 600
thin solid films
www.elsevier.com/locate/tsf

Small helicon plasma source for electric propulsion

K. Toki [a,*], S. Shinohara [b], T. Tanikawa [c], K.P. Shamrai [d]

[a] *Mechanical Systems Engineering, Tokyo University of Agriculture and Technology, 2-24-16 Naka-cho Koganei-city Tokyo 184-8588, Japan*
[b] *Interdisciplinary Graduate School of Engineering Sciences, Kyushu University, 6-1 Kasuga-Kohen, Kausga, Fukuoka 816-8580, Japan*
[c] *Research Institute of Science and Technology, Tokai University, 2-28-4 Tomigaya, Shibuya-ku, Tokyo 151-8677, Japan*
[d] *Institute for Nuclear Research, National Academy of Sciences, 47 Prospect Nauki, Kiev 03680, Ukraine*

Available online 19 September 2005

Abstract

An investigation was conducted for a very small helicon plasma source of a 2.5 cm i.d. glass tube. Since the operational features of electric propulsion are determined by its plasma density and degree of ionization, the helicon plasma including inductively coupled plasma (ICP) has a niche requirement as high as 10^{13} cm^{-3} density at the optimized condition of both RF frequency and applied magnetic field. In this paper, by using Ar, the RF frequency was scanned from 27.12 up to 67.80 MHz and the applied magnetic field was moderately varied from 0 to about 0.01 T. The maximum input power was 250 W at this time and 8×10^{12} cm^{-3} was achieved.

Keywords: Helicon plasma source; Electric propulsion; Electrodeless discharge; Electromagnetic acceleration

1. Introduction

Helicon plasma sources have been intensively studied as the high density plasma sources up to 10^{13} cm^{-3} or higher [1,2] and also as the engineering of non-resonant devices with easier applications to plasma processing. In this study the major purpose is focused into smaller sizes of 2.5 cm i.d. glass tube with its straight portion length of 80 cm [3]. This has a full opening end to the vacuum. Very large helicon plasma sources up to 75 cm i.d. are simultaneously studied by our group at another place for physics and space plasma simulation [4–7]; however, smaller applications are more difficult for the electric propulsion from the viewpoint of plasma loss at the wall. If the small size application would be successful, the larger size application becomes more feasible. Therefore, our target is to produce 10^{13} cm^{-3} plasmas for Ar gas in the above glass tubes. It would be the world smallest helicon plasma when the condition is identified as the helicon mode.

Another motivation of this study is to investigate the electromagnetic acceleration of produced plasma. There exist a few electrodeless electric propulsions where the plasma production is free from the electrode erosion, consequently the lifetime limitation due to the material losses. In the acceleration phase, no electrodeless acceleration was achieved, and that part is inevitably eroded or sputtered due to the direct contact with plasma flow impingement. We are proposing a new type of electromagnetic acceleration method by induced current and applied magnetic field. This idea is pulsed acceleration, applying repetitive profile of current to a multi-turns coil around the glass tube. Finally, this method is to be confirmed experimentally.

2. Experimental set-up

2.1. Experimental devices

A 2.5 cm i.d. Pyrex glass tube is connected with a plastic joint through a Pyrex glass reducer to a steel vacuum chamber of 1.2 m in diameter and 2 m in length evacuated by a rotary pump and a mechanical booster pump. The pressure inside the glass tube at the antenna was about 15 mTorr for 0.5 mg/s (=17 sccm), 30 mTorr for 1 mg/s (=34 sccm), 50 mTorr for 2 mg/s (=68 sccm), 80 mTorr for 4 mg/s (=136 sccm) flow rates of Ar. A signal generator of KENWOOD SG-5150, an RF-post-amplifier of THAMWAY T142-4749A and a main amplifier of THAMWAY T145-5768A with a matching box of THAMWAY T020-5558A were used for RF power source capable of generating 0–250 W at the frequency range of 27.12–67.80 MHz. A directional coupler inside the matching box monitors

* Corresponding author.
E-mail address: toki@cc.tuat.ac.jp (K. Toki).

0040-6090/$ - see front matter © 2005 Elsevier B.V. All rights reserved.
doi:10.1016/j.tsf.2005.08.039

the antenna loading of the forward/reverse power and a Pearson current sensor/capacitive voltage monitor measures the antenna current and voltage. A solenoid coil of about 250 turns having an i.d. of 10 cm and a length of 14 cm produces 5 G/A uniform and almost axial magnetic field at the helicon plasma source. This solenoid coil is separate from an acceleration coil with radially expanding magnetic field having a function of pulsed electromagnetic acceleration at the downstream portion of the helicon plasma source. The typical experimental set-up (acceleration coil is discarded) is depicted in Fig. 1 and the produced Ar plasma was photographed in Fig. 2.

A set of double probe was used to measure the plasma density and electron temperature. A pair of 0.3 mm diameter tungsten wires was exposed at the tip of 4 mm from a 2 mm diameter ceramic tube. This probe was inserted to the center of the antenna location in the midst of plasma production. The probe biasing voltage and polarity were determined by ±100 V bipolar electrical power source to sweep the probe voltage from −40 V to 40 V. The probe voltage and current were read out by electrically floating multi-meters. As is often recognized in the RF plasmas, the probe curve is skewed except for the ion saturation and very beginning of the electron current portions. Sometimes sophisticated measurements system such as synchronized sweep with the applied RF frequency to trace a single probe curve by using lock-in amplifier and an RF compensation probe are employed; however, in this experiment, the plasma temperature was evaluated from the very vicinity of the ion saturation portion.

2.2. Description of small helicon plasma source

As already mentioned, we designed a glass tube plasma source, 80 cm long including 2×90° bents with a fully opened end to vacuum through a glass reducer with a diameter of about 20 cm. This tube uses Pyrex glass having dimensions of 2.5 cm i.d. and 3.4 cm o.d. The tube has a grounded metal end plate with a propellant inlet port for Ar or other gases. We employed a simple double-loop parallel antenna having a copper strip width of 16 mm, the loop spacing of 8 mm, and the strip thickness of 0.1 mm. The double-loop parallel antenna is wound in the straight portion near the upstream gas port.

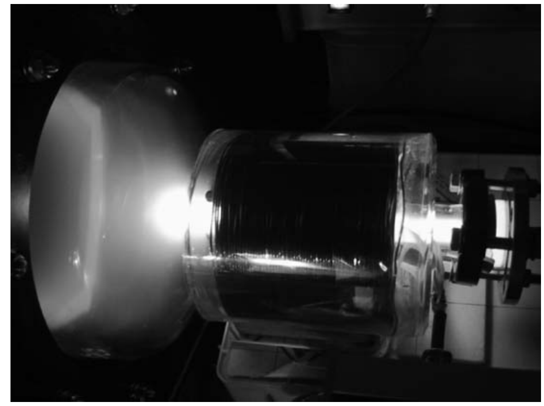

Fig. 2. Photograph of Ar plasma at ignition.

2.3. Electromagnetic acceleration region

Since the acceleration electrodes of electric propulsion usually suffer from erosion caused by plasma impingement, for example, the grid of ion thruster, the cathode of MPD thruster, etc., we already proposed an erosion free acceleration method. It basically requires azimuthally induced current j_θ inside the plasma, interacting with the radial component B_r of diverging magnetic fields B to produce $j_\theta \times B_r$ acceleration

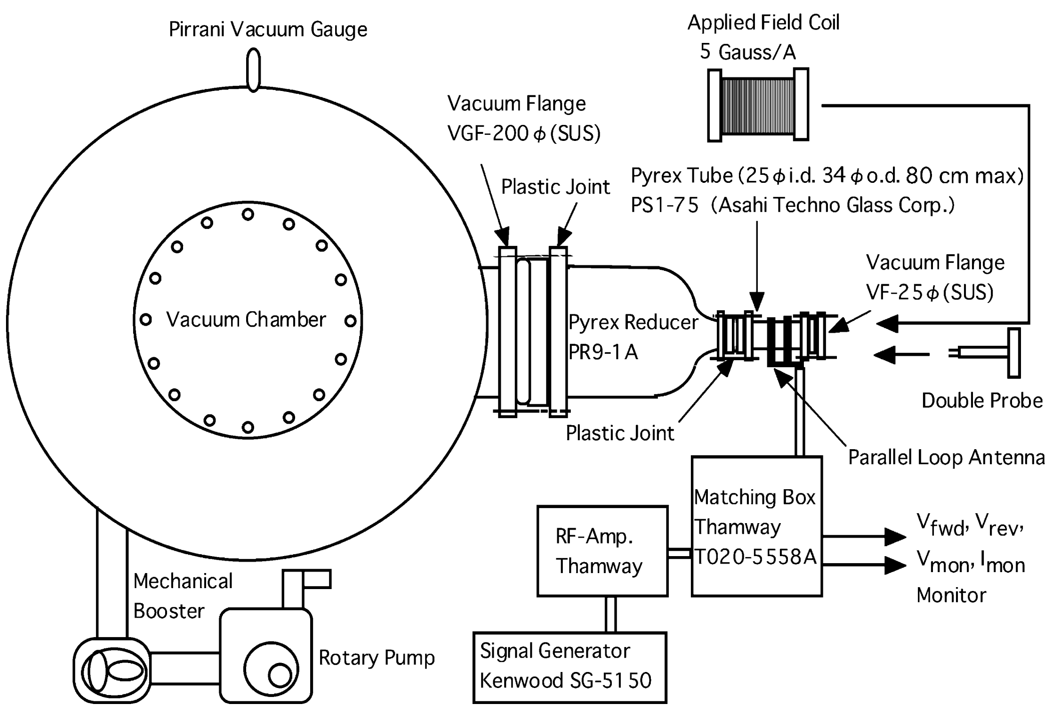

Fig. 1. Experimental set-up.

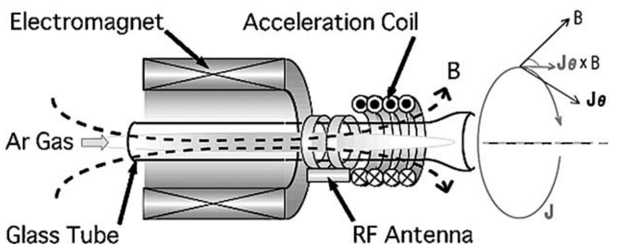

Fig. 3. Principle of pulsed electromagnetic acceleration proposed by Shinohara.

force [3]. This method is pulsed electromagnetic field force acceleration proposed by Shinohara and resembles the Pulsed Inductive Thruster (PIT) studied by Mikellides [8]. But the most different feature is repetitive pulses and a separate coil for acceleration. Fortunately, the small helicon plasma source has a coil for the externally applied magnetic field expanding toward downstream region where the coil for acceleration is wound as shown in Fig. 3. A circuit analysis shows that the rapid change of coil current induces larger electromotive force in the right-hand side of Eq. (1) and consequently a stronger I_p inside the plasma.

$$L_p \frac{dI_p}{dt} + R_p I_p = V_{ext} \quad (1)$$

L_p: plasma inductance, R_p: plasma resistance, I_p: induced plasma current, V_{ext}: induced voltage by the varying applied field.

3. Experimental results

3.1. Frequency selection

In order to select the RF frequency, we evaluated the minimum ignition power from the starting frequency of 13.56 MHz until 81.36 MHz at every 13.56 MHz step. As shown in Fig. 4, the plasma ignition power becomes almost the minimum, less than 25 W, ranging from 27.12 MHz to 67.80 MHz. We selected in this experiment the frequency of 67.8 MHz where the plasma ignition occurs at less than 10 W RF input power. This frequency is comparable to the collision frequency of about 50 MHz between the electrons and neutrals before ignition.

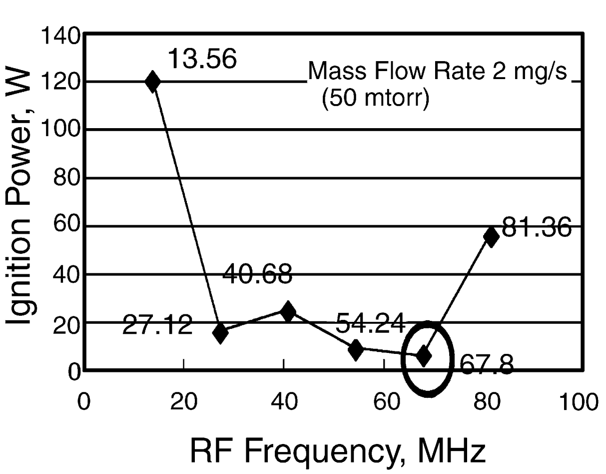

Fig. 4. RF frequency selection according to the minimum ignition power.

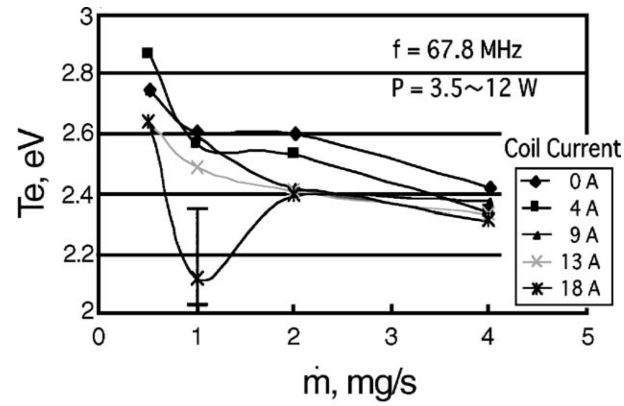

Fig. 5. Electron temperature vs. Ar mass flow rate with various applied magnetic fields.

3.2. Electron temperature vs. mass flow rate

Fig. 5 shows the electron temperature vs. Ar mass flow rate by using a double probe at the midst of plasma production region, the center of double loop parallel antenna. In this case the RF input power is low near the ignition power of 3.5–12 W. The electron temperature exhibited monotonous decrease from 3 to 2.5 eV with increasing mass flow rate from 0.5 to 4 mg/s and slight decrease with increasing applied magnetic field strength. The electron temperature at 18 A coil current involves a large error due to noise effect to the probe.

3.3. Plasma density vs. mass flow rate

At the same RF input power range, the ion density was also determined from the double probe measurement as shown in Fig. 6. The plasma density rapidly increased with mass flow rates from 0.5 to 1 mg/s but at higher flow rates than 1 mg/s, it was almost saturated and slightly increased toward 10^{12} cm^{-3}.

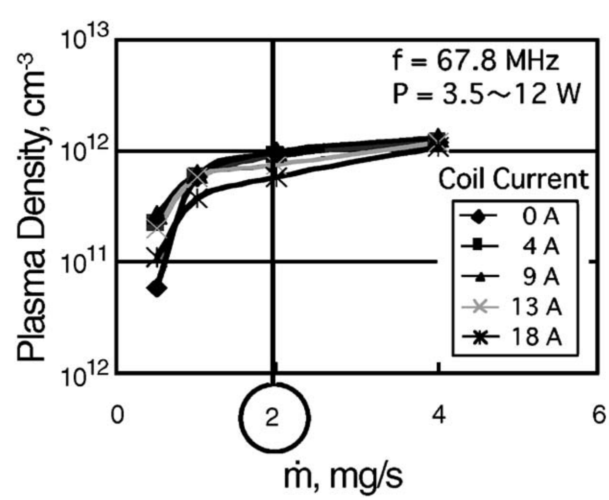

Fig. 6. Plasma density vs. Ar mass flow rate with various applied magnetic fields.

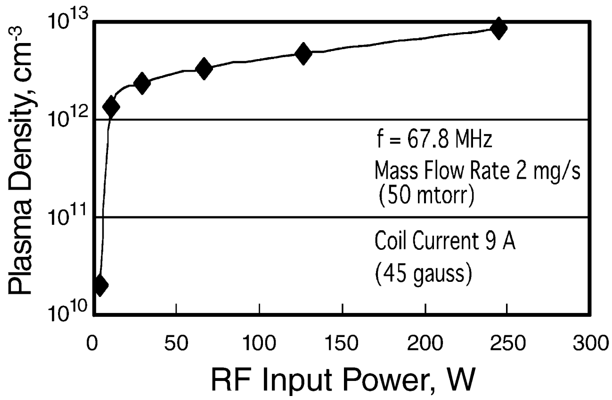

Fig. 7. Plasma density vs. RF input power under the applied magnetic field of 45 G.

This tendency together with the electron temperature decrease suggests that the electron energy transfers efficiently to the neutrals because of the pressure/density rise inside the glass tube with increasing mass flow rates. The effect of the magnetic field strength was not so significant except at the lowest mass flow rate of 0.5 mg/s and the maximum magnetic field strength did not correspond to the highest plasma density. This might imply that the slight change took place in the matching condition of the RF input under applied magnetic fields.

3.4. Plasma density vs. RF input power

Finally, the plasma density vs. the RF input power was plotted in Fig. 7 under the selected mass flow rate of 2 mg/s and the applied magnetic field strength of 9 A (=45 G). From this graph, we can find the plasma density rapidly increased from 10^{10} cm^{-3} at 10 W ignition to 10^{12} cm^{-3} at 20 W RF input power, however, beyond this level toward 250 W, the density increase was quite slow up to 8×10^{12} cm^{-3}. The abrupt density increase at low power level might correspond to the CCP (Capacitively Coupled Plasma) to ICP (Inductively Coupled Plasma) mode transition of plasma production, and after this point a helicon jump was originally expected but not observed or remained within a quite moderate jump.

4. Conclusion

Relatively high density Ar plasma of 8×10^{12} cm^{-3} was obtained at 250 W RF input power by a double loop antenna applied to a small helicon plasma source of 2.5 cm i.d. and 80 cm in length with an open end to the vacuum chamber. The density was slightly lower than the targeted value of 10^{13} cm^{-3}, suitable for electromagnetic acceleration of the electric propulsion. This is due to the limitation of experimental survey at present. The mass flow rate reduction down to 1 mg/s is necessary under 10 mTorr pressure without ambient gas effect under the sufficient magnetic field strength up to 200 G. The saddle type or helical type antennae should be compared to the double loop antenna.

Acknowledgement

This work is supported by a Grant-in-Aid for Scientific Research (B) of Japan Society for the Promotion of Science (JSPS).

References

[1] R. Boswell, Plasma Phys. Control. Fusion 26 (1984) 1147.
[2] F.F. Chen, Plasma Phys. Control. Fusion 33 (1991) 339.
[3] K. Toki, S. Shinohara, T. Tanikawa, I. Funaki, K.P. Shamrai, IEPC 03-1168, the 28th International Electric Propulsion Conference, Toulouse, France, March 17–21, 2003.
[4] S. Shinohara, T. Tanikawa, Topic No. 6, XXI International Congress on Phenomena in Ionized Gases, Greifswald, Germany, 2003.
[5] S. Shinohara, T. Tanikawa, Rev. Sci. Instrum. 75 (2004) 1941.
[6] T. Tanikawa, S. Shinohara, S. Sato, Y. Nakamura, Bull. Am. Phys. Soc. 47 (2002) 47.
[7] K.P. Shamrai, S. Shinohara, 7th Asia Pacific Conference on Plasma Science and Technology, Topic No. 13, Fukuoka, Japan, 2004.
[8] P.G. Mikellides, IEPC 03-0135, the 28th International Electric Propulsion Conference, Toulouse, France, March 17–21, 2003.